Journal of King Saud University – Science 35 (2023) 102585

HOSTED BY

Contents lists available at ScienceDirect

Journal of King Saud University – Science

journal homepage: www.sciencedirect.com

Original article

Protocatechuic acid mitigates CuO nanoparticles-induced toxicity by strengthening the antioxidant defense system and suppressing apoptosis in liver cells

Maqusood Ahamed [a,*], Mohd Javed Akhtar [a], M.A. Majeed Khan [a], Hisham A. Alhadlaq [a,b]

[a] King Abdullah Institute for Nanotechnology, King Saud University, Riyadh 11451, Saudi Arabia
[b] Department of Physics and Astronomy, College of Science, King Saud University, Riyadh 11451, Saudi Arabia

ARTICLE INFO

Article history:
Received 10 November 2022
Revised 24 November 2022
Accepted 30 January 2023
Available online 3 February 2023

Keywords:
Protocatechuic acid
CuO NPs
Liver cells
Antioxidants
Apoptosis
Cytoprotective mechanism

ABSTRACT

Due to exceptional properties, copper oxide nanoparticles (CuO NPs) are now being applied in diverse fields such as agriculture, cosmetics, food industry, and medicine. There is enough scientific evidence that CuO NPs are toxic to living organisms. However, no effective method is available to mitigate the health hazard of the CuO NPs. This study aimed to investigate the possible cytoprotective mechanism of protocatechuic acid (PCA) from the toxicity of CuO NPs in human liver HepG2 cells and primary rat hepatocytes. CuO NPs were synthesized by a facile hydrothermal method. X-ray diffraction and electron microscopy characterization data confirmed the formation of spherical and crystalline CuO NPs with smooth surface morphology. On the basis of preliminary results, cells are divided into four groups; (i) control group, (ii) PCA group (10 μg/mL, a non-cytotoxic dose), (iii) CuO NPs group (IC_{50}), and (iv) co-exposure group (PCA + CuO NPs). Results show that pre-treatment with PCA significantly abrogates the CuO NPs-induced cytotoxicity and lactate dehydrogenase leakage in both types of cells. CuO NPs-induced reactive oxygen species, hydrogen peroxide, and malondialdehyde levels are remarkably mitigated by the PCA pre-treatment. The depletion in glutathione and several antioxidant enzymes (e.g. glutathione peroxidase, superoxide dismutase, and catalase) because of the CuO NPs exposure is effectively restored by PCA. Caspase-3 gene up-regulation and mitochondrial membrane potential depletion due to CuO NPs exposure are also alleviated by the pre-treatment using PCA. Therefore, this first study reports the mitigating potential of PCA against CuO NPs toxicity in liver cells by restoring the antioxidant defense system and quashing the apoptosis.

1. Introduction

Copper oxide nanoparticles (CuO NPs) have received great attention for various applications because of their unique thermal, electrical and optical properties (Islam et al., 2020). Due to the unique physicochemical characteristics, CuO NPs are used in diverse fields, including gas sensor, solar cell, catalysis, agriculture, cosmetics, paints, textiles, environmental remediation, food industry, and biomedical purposes (Khalaj et al., 2018). It is estimated that from 2020 to 2025 the world will consume approximately 200–830 tons of CuO NPs each year (Ahamed et al., 2022a). The huge demand and diverse application of CuO NPs will significantly enhance the possibility of their discharge into the environment and cause potential hazards to human health and the eco-system (Bialy et al., 2020).

The toxicological potential of CuO NPs has been comprehensively studied in a series of cultured cells, and *in vivo* models. CuO NPs can be toxic to various mammalian cells including lung, skin, breast, brain, kidney, neuronal, intestine, and liver cells, using oxidative stress pathways (Abudayyak et al, 2020; Fahmy et al., 2020). A recent *in vivo* study demonstrated that an oral dose of CuO NPs induces toxicity in the hepatic, renal, and splenic tissue of mice (Bialy et al., 2020). Another study observed that the oral exposure of rats to CuO NPs induces liver toxicity by free radical generation (Anreddy, 2018). Toxicity of CuO NPs was also found in non-mammalian *in vivo* systems. For example, oral exposure

* Corresponding author.
E-mail address: mahamed@ksu.edu.sa (M. Ahamed).
Peer review under responsibility of King Saud University.

Production and hosting by Elsevier

https://doi.org/10.1016/j.jksus.2023.102585
1018-3647/

of CuO NPs disrupts the gut homeostasis of *Drosophila melanogaster*, and redox imbalance was one of the crucial causes of toxicity (Baeg et al., 2018).

There is no effective method for reducing the CuO NPs exposure; hence, humans can be regularly exposed to CuO NPs from the workplace, environment, and contaminated food and water. It is a relevant concern of researchers to develop new methods to minimize the hazardous effects of CuO NPs in humans. CuO NP toxicity is closely linked with redox imbalance, the supplementation of antioxidants, as a therapeutic strategy, might be a possible way to attenuate CuO NPs-induced toxicity in humans. Protocatechuic acid (PCA, 3,4-dihydroxybenzoic acid) can prevent the toxic effects of CuO NPs. PCA is a kind of phenolic compound widely present in several edible nuts, vegetables, and fruits, and it is easily absorbed by animals and humans (Antony and Wasewar, 2020; Owumi et al., 2019). PCA has shown several biological activities, including antibacterial, antidiabetic, antioxidant, and anti-inflammatory properties (Antony and Wasewar, 2020; Semaming et al., 2015). Moreover, PCA has a structural resemblance with caffeic acid, gallic acid, and vanillic acid, which are known for antioxidant activities (Kakkar and Bais, 2014). There is growing evidence showing that the pharmacological activities of PCA are closely linked with the mitigation of redox imbalance, inflammation, and apoptosis (Semaming et al., 2015). A recent finding indicated that PCA mitigates Cd-induced neurotoxicity in rats using its antioxidant activity (AlOlayan et al., 2020).

PCA is investigated for possible therapeutic actions against several human ailments; however, data are scarce on its protective mechanisms against metal oxide NPs-induced toxicity. The liver is one of the most targeted organs of metal oxide NPs after they enter the body through any possible route (Lee et al., 2016). Hence, this work was planned to study the cytoprotective effects of PCA from CuO NPs-induced toxicity in human liver cells (HepG2) and primary rat hepatocytes. The possible mitigating mechanism of PCA from CuO NPs induced toxicity was also delineated using oxidative stress and apoptosis pathways.

2. Materials and methods

2.1. Synthesis and characterization of CuO NPs

CuO NPs was prepared by a simple hydrothermal method using copper nitrate ($CuNO_3{\cdot}2H_2O$) (Sigma-Aldrich, St. Louis, MO, USA) and sodium hydroxide (NaOH) (Ahamed et al., 2022a, 2022b). The phase purity and crystalline nature of CuO NPs were assessed by X-ray diffraction (XRD) (PanAnalytic X'Pert Pro) (Malvern Instruments, WR14 1XZ, UK) using Cu-Kα radiation (λ = 0.154 nm at 45 kV and 40 mA). Structural characterization was further done by field emission scanning electron microscopy (FESEM, JSM-7600F, JEOL, Inc., Tokyo, Japan) and field emission transmission electron microscopy (FETEM, JEM-2100F, JEOL).

The hydrodynamic size and zeta potential of CuO NPs and CuO NPs + PCA suspensions in distilled water and complete culture medium (DMEM + 10 %FBS) were examined by dynamic light scattering (DLS) (ZetaSizer Nano-HT, Malvern Instruments). CuO NPs (IC_{50}) and CuO NPs (IC_{50}) + PCA (10 μg/mL) were suspended in distilled water and culture media. Subsequently, the suspensions were sonicated for 15 min at 40 W using a water bath sonicator and DLS experiment was performed.

2.2. Cell culture

HepG2 cell line was purchased from American Type Culture Collection (ATCC) (Manassas, VA, USA). Primary rat hepatocytes were isolated by a collagenase perfusion procedure as reported by Moldeus and co-workers (Moldeus et al., 1978). Cells were grown in Dulbecco's modified eagle's medium (DMEM) (Invitrogen, Carlsbad, CA, USA) or Roswell Park Memorial Institute (RPMI) 1640 medium (Sigma-Aldrich) supplemented with streptomycin (100 μg/mL, Invitrogen) and penicillin (100 U/mL, Invitrogen), and 10 % fetal bovine serum (FBS, Invitrogen). The cells were maintained with 5 % CO_2 supply at 37 °C in a humidified incubator.

2.3. Exposure protocol and selection of the appropriate concentrations of CuO NPs and PCA

Sock solution (1 mg/mL) of synthesized CuO NPs and purchased PCA (Sigma-Aldrich) was prepared in culture medium. First, we performed a screening 3-(4,5-dimethylthiazol-2-yl)-2,5-diphenylt etrazolium bromide (MTT) assay to choose the appropriate dosages of CuO NPs and PCA. HepG2 cells and primary rat hepatocytes were individually treated to various concentrations of CuO NPs (0, 1, 2.5, 5, 10, 25, 50, and 100 μg/mL) and PCA (0, 1, 2.5, 5, 10, 25, 50, and 100 μg/mL) for 24 h. Results showed that PCA did not induce cytotoxicity in the selected concentrations in both types of cells (Fig. S1, Supplementary material). Conversely, CuO NPs induced dose-dependent cytotoxicity in the concentration range of 5–100 μg/mL in both types of cells (Fig. S3, Supplementary material). The IC_{50} values of CuO NPs were 26.56 μg/mL and 29.66 μg/mL for HepG2 cells and primary rat hepatocytes, respectively (Fig. S3, Supplementary material). Therefore, in co-exposure experiments we have the selected IC_{50} value of CuO NPs. To further choose the appropriate concentration of PCA, we performed experiments where different concentrations of PCA (1–100 μg/mL) are co-exposed with the IC_{50} value of CuO NPs (Fig. S4, Supplementary material). Results showed that cell viability declined to approximately 50 % following the exposure to CuO NPs (IC_{50}), and treatment with PCA increased the cell viability in a dose-dependent manner in the concentration range of 1–10 μg/mL. Hence, our data suggested that treatment with PCA at the concentration of 10 μg/mL achieved maximum mitigating effect against CuO NPs (IC_{50}) induced cytotoxicity in both cells. This indicated that 10 μg/mL PCA was enough to mitigate the IC_{50} toxicity of CuO NPs (Fig. S4, Supplementary material). Hence, for this study, we utilized 10 μg/mL of PCA to explore its mitigating potential against CuO NPs (IC_{50}) induced toxicity. The cells were divided into four groups; control group, PCA group (10 μg/mL), CuO NPs group (IC_{50}), and co-exposure group (PCA + CuO NPs). In the co-exposure group, 10 μg/mL of PCA was exposed to cells 30 min before the treatment of CuO NPs (IC_{50}). Exposure time in all experiments was 24 h.

2.4. Biochemical parameters

MTT assay (Mosmann, 1983) with few modifications (Ahamed et al., 2011) was applied to measure cell viability. Lactate dehydrogenase (LDH) enzyme leakage from cytoplasm to culture media after membrane disintegration was assayed as described earlier (Welder, 1992). The cell morphology of the control and treated cells was captured using a phase-contrast microscope (Leica Microsystems, GmbH, Wetzlar, Germany). Images were grabbed at 20 × magnification. Red-orange cationic fluorescent dye tetramethylrhodamine, metyl ester, perchlorate (TMRM) (Thermo Fisher Scientific, Waltham, MA, USA) is rapidly taken up by mitochondria in a potential dependent manner. Hence, TMRM probe was applied to assess the mitochondrial membrane potential (MMP) level in treated and control cells. MMP level was determined by two different methods; quantification by a microplate reader (excitation/emission wavelength: 548/574 nm) (Synergy-HT, BioTek, Winooski, VT, USA) and the intracellular brightness of TMRM was captured using a DMi8 fluorescent microscope using green excitation filter (detecting red-yellow TMRM emission) (Leica

Microsystems, GmbH, Wetzlar, Germany). Probe 2,7-dichlorofluorescein diacetate (DCFH-DA, Sigma-Aldrich) was utilized to measure the intracellular level of reactive oxygen species (ROS) as reported earlier (Siddiqui et al., 2013). The quantitative analysis of ROS was performed using a microplate reader (excitation/emission wavelength: 485/520 nm) (Synergy-HT, BioTek). The fluorescent images of intracellular ROS were also capture using a DMi8 fluorescent microscope using blue excitation filter (detecting green DCF emission) (Leica Microsystems). The fluorometric assay of intracellular hydrogen peroxide (H_2O_2) was performed using a commercial kit (MAK164 green fluorescence, Sigma-Aldrich). The fluorometric assay of the caspase-3 enzyme was carried out using the 7-amido-4-trifluoromethylcoumarin (AFC) standard (Akhtar et al., 2020). The expression level of the mRNA of the caspase-3 gene (CASP-3) was determined using a real-time polymerase chain reaction (PCR, ABI PRISM, 7900HT Sequence Detection System) (Applied Biosystems, Foster City, CA, USA) according to the procedures described earlier (Ahamed et al., 2011). Malondialdehyde (MDA), an end product of lipid peroxidation was determined using methods in a previous study (Ohkawa et al., 1979). Glutathione (GSH) level was quantified using Ellman's method (Ellman, 1959). The activity of the glutathione peroxidase (GPx) enzyme was measured using the protocol of Rotruck and coworkers (Rotruck et al., 1973). The enzymatic activity of catalase was assayed according to the procedure of Sinha et al. (Sinha, 1972). The colorimetric assay of superoxide dismutase (SOD) enzyme was carried out using a kit from Cayman Chemical Company (Ann Arbor, MI, USA). Protein content was quantified using Bradford's protocol (Bradford, 1976).

2.5. Statistical analysis

One-way analysis of variance (ANOVA) followed by Dennett's multiple comparison tests was applied for the analysis of results. The $p < 0.05$ was assigned as statistically significant. All the quantitative data presented in this study were mean ± SD of five independent experiments (n = 5).

3. Results

3.1. Characterization of CuO NPs

The XRD pattern of prepared CuO NPs is shown in Fig. 1A. All the diffraction peaks noticed at 2θ were matching to the planes (−110), (002), (111), (−202), (020), (202), (−113), (−311), (320), (311), and (22–) that were matched with Joint Committee on Powder Diffraction Standards (JCPDS) card no. 45–0937, indicating the monoclinic structure of CuO NPs (Arun et al., 2020). The particle size of the CuO NPs was estimated from the strongest peak (111), applying Scherrer's formula. The average particle size of the CuO NPs was approximately 33 nm. Impurity peaks were not detected, which further confirmed the purity of the synthesized CuO NPs. The high intensity of the peaks indicates the high crystallinity of the prepared CuO NPs. FESEM (Fig. 1B) and FETEM (Fig. 1C) micrographs indicated that the prepared CuO NPs had spherical morphology with smooth surfaces. The average particle size calculated from TEM (>100 NPs) was approximately 31 nm, which corresponded with the XRD results. In the high-resolution TEM micrograph (Fig. 1D), the calculated inter-planner distance was 0.254 nm, corresponds to the (002) plane and is consistent with the monoclinic structure of the CuO phase.

The DLS study showed that the hydrodynamic size of the CuO NPs was several times larger than that determined by XRD and TEM (Table 1). The relatively large size of the NPs in the aqueous medium was due to the agglomeration of the NPs. Zeta potential values (26–30 eV) showed that the CuO NPs suspensions were fairly stable in distilled water and culture media. Zeta potential data further indicated that the CuO NPs suspended in water displayed a positive surface charge, while that in complete culture media (DMEM + 10 % FBS) exhibited a negative surface charge. The negative surface charge of the CuO NPs in the culture medium might be due to the adsorption of negatively charged proteins on the surface of CuO NPs. The presence of PCA in the CuO NPs suspension in distilled water and culture medium did not affect the aqueous behavior of CuO NPs.

3.2. PCA mitigates CuO NPs-induced cytotoxicity in HepG2 cells

HepG2 cells were exposed for 24 h to CuO NPs (IC_{50}) and/or PCA (10 μg/mL, a non-cytotoxic concentration) and cytotoxicity was assessed. Fig. 2A shows that the CuO NPs-induced cell viability reduction was significantly increased by the PCA pre-treatment ($p < 0.05$). Fig. 2B shows that the CuO NPs exposure significantly increased LDH leakage, but these changes were effectively reverted by the PCA pre-treatment. Fig. 3C depicts the morphology of HepG2 cells in control and experimental groups. CuO NPs treated group showed unhealthy cells and relatively low cell density. However, PCA pre-treatment resulted in remarkable improvement in the morphology and density of the CuO NPs treated cells.

3.3. PCA mitigates CuO NPs-induced oxidative stress in HepG2 cells

HepG2 cells were exposed to CuO NPs and/or PCA for 24 h, and oxidative stress response was evaluated by determining the various parameters of the pro-oxidants and antioxidants. Fluorescent microscopy images suggested that the brightness of the dichlorofluorescein (DCF) probe increased (an indicator of ROS generation) in the CuO NPs treated cells, and the pre-treatment of the PCA remarkably reduced the ROS generation as the brightness of the DCF probe decreased in the PCA + CuO NPs group (Fig. 3A). Similarly, quantitative data indicated that the increment in the intracellular ROS level because of the CuO NPs exposure was significantly attenuated by the PCA pre-treatment ($p < 0.05$) (Fig. 3B). Moreover, the CuO NPs-induced H_2O_2 (pro-oxidant) and MDA (an end product of lipid peroxidation) levels were effectively abrogated by PCA ($p < 0.05$) (Fig. 3C and D). The mitigating potential of PCA against CuO NPs-induced antioxidants depletion was further examined in HepG2 cells. Results demonstrated that the GSH level and activity of antioxidant enzymes (GPx, SOD, and CAT) were lower in the CuO NPs treated group than in the control group ($p < 0.05$). Additionally, the CuO NPs-induced antioxidant depletion was restored by the PCA pre-treatment ($p < 0.05$) (Fig. 4A-D).

3.4. PCA mitigates CuO NPs induced apoptosis in HepG2 cells

HepG2 cells were treated to CuO NPs and/or PCA for 24 h, and the apoptotic response was assessed by measuring the MMP level and regulation of the caspase-3 gene. Fluorescent microscopy data showed that the brightness of the TMRM probe decreased (an indicator of MMP reduction) in the CuO NPs treated cells, and the pre-treatment of PCA significantly increased the brightness of the TMRM probe (an indicator of MMP gain) (Fig. 5A). Likewise, the quantitative analysis of MMP showed that the CuO NPs-induced MMP loss was significantly mitigated by PCA ($p < 0.05$) (Fig. 5B). Real-time PCR data demonstrated that the down-regulation of the caspase-3 gene (mRNA level) due to the CuO NPs exposure was significantly reverted by the PCA pretreatment (Fig. 5C). To support the mRNA data, the activity of the caspase-3 enzyme was further examined in HepG2 cells following the exposure to CuO NPs and/or PCA for 24 h. In agreement with the mRNA data,

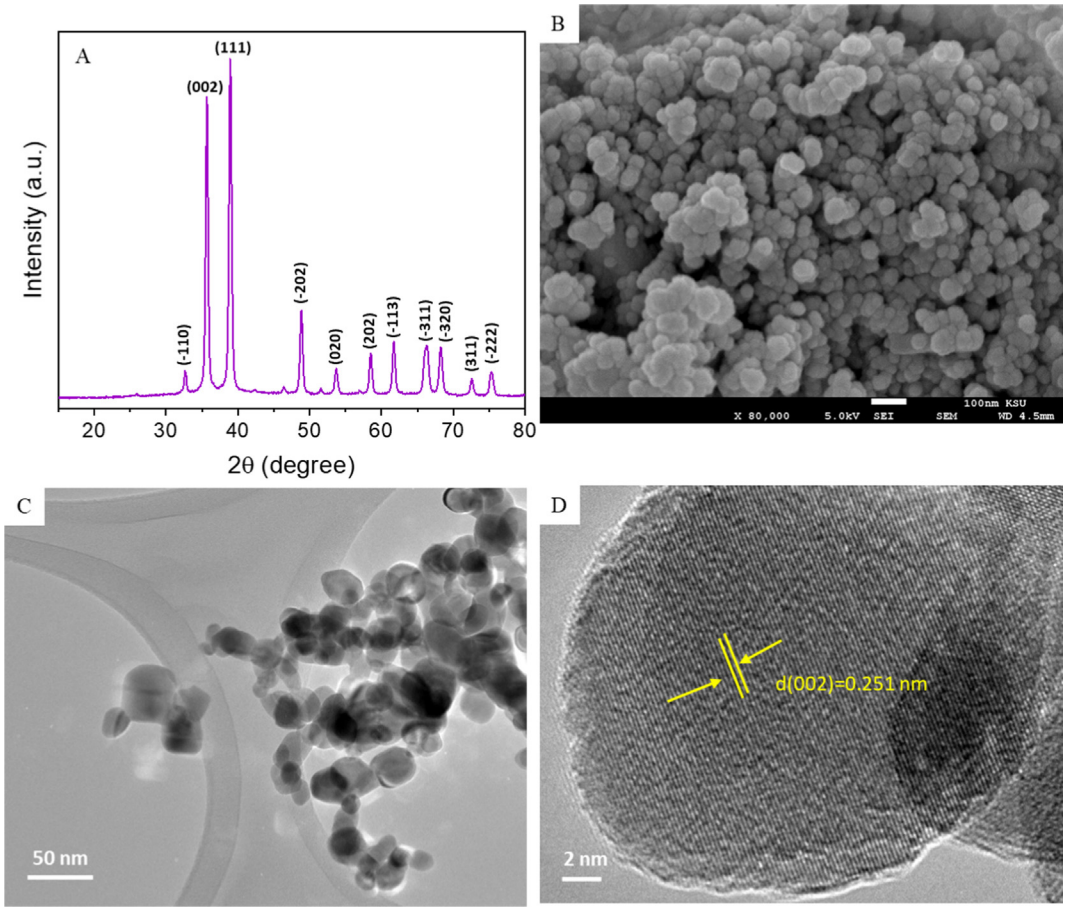

Fig. 1. Characterization of CuO NPs. (A) XRD spectra, (B), SEM micrograph, (C) Low resolution TEM micrograph, and (D) High resolution TEM micrograph.

Table 1
Dynamic light scattering characterization of CuO NPs. Data are presented as mean ± SD of three independent experiment (n = 3).

Parameters	Hydrodynamic size (nm)		Zeta potential (mV)	
	Distilled water	Culture medium	Distilled water	Culture medium
CuO NPs	97.46 ± 4.56	113.53 ± 4.83	27.45 ± 1.24	−26.36 ± 1.31
CuO NPs + PCA	93.57 ± 3.87	105.26 ± 4.37	29.23 ± 1.17	−30.43 ± 1.08

the CuO NPs induced caspase-3 enzyme activity was effectively ameliorated by PCA (Fig. 5D).

3.5. PCA mitigates CuO NPs-induced cytotoxicity, oxidative stress, and apoptosis in primary rat hepatocytes

The protective effects of PCA against CuO NPs-induced toxicity were further explored in primary rat hepatocytes. The cells were treated for 24 h to CuO NPs (IC_{50} = 29.66 μg/mL) and/or PCA (10 μg/mL). Results showed that the CuO NPs induced cell viability reduction and LDH leakage were significantly alleviated by PCA pre-treatment ($p < 0.05$ for each) (Fig. 6A and B). The CuO NPs induced ROS generation and GSH depletion were also remarkably attenuated by PCA ($p < 0.05$ for each) (Fig. 6C and D). The alleviating potential of PCA from CuO NPs induced apoptosis was further explored in primary rat hepatocytes by measuring the MMP level and caspase-3 enzyme activity. We observed that the CuO NPs induced MMP loss and caspase-3 enzyme activation was significantly suppressed by pre-treatment of PCA ($p < 0.05$ for each) (Fig. 7A and B). In agreement with the HepG2 cells data, these results also indicated the cytoprotective effects of PCA against CuO NPs-induced toxicity in primary rat hepatocytes.

4. Discussion

Due to their tiny size and surface characteristics, metal oxide NPs may cross cell/tissue barriers and accumulate in different vital organs. CuO NPs are one of the most biologically reactive metal oxide NPs (Ahamed et al., 2015; Moschini et al., 2013). Several *in vitro* and *in vivo* studies reported the toxicity of CuO NPs in the liver (Abdelazeim et al., 2020; Siddiqui et al., 2013). However, no effective method is known to reduce the CuO NPs toxicity once they enter the human body. This novel study demonstrated the alleviating potential of PCA against the CuO NPs-induced toxicity in liver cells. Results showed that the CuO NPs-induced cytotoxicity in human liver (HepG2) cells and primary rat hepatocytes was remarkably mitigated by PCA pre-treatment. LDH enzyme is located in the cytoplasm of the cell, which is close to the cell membrane. Hence, slight damages in the cell membrane will result in LDH enzyme leakage into the extracellular fluid e.g., the culture media. The relatively high LDH activity following the CuO NPs

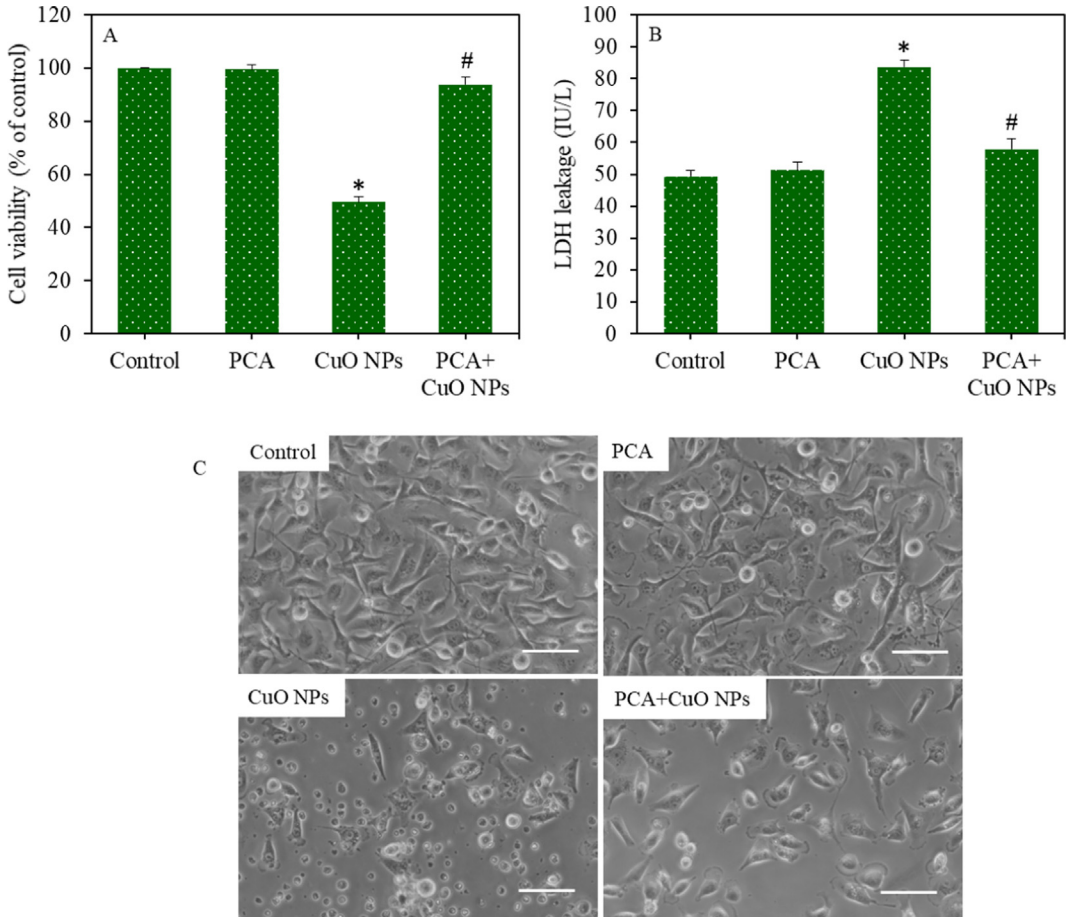

Fig. 2. Cytotoxicity of HepG2 cells following exposure to the CuO NPs (IC_{50}) and/or PCA (10 μg/mL) for 24 h. (A) MTT cell viability. (B) LDH enzyme leakage. (C) Cellular morphology (scale bar represents 50 μm). *statistically significant difference from the control group ($p < 0.05$). #statistically significant difference from the CuO NPs group ($p < 0.05$).

exposure in the HepG2 cells and primary rat hepatocytes in the present study indicated the altered cell membrane permeability with the consequences of its leakage from the cytoplasm to the culture media. However, LDH activity was significantly decreased by the PCA pre-treatment suggesting the cytoprotective role of PCA against the CuO NPs-induced toxicity in liver cells. Earlier studies demonstrated the protective effects of PCA against heavy metals (e.g., Cd) and antitumor drugs (e.g., cisplatin) induced toxicity in rats (Owumi et al., 2019).

Oxidative stress due to the excessive production of ROS has been involved in the pathogenesis of liver diseases (Ahamed et al., 2015; Ahamed et al., 2022b). Although ROS is normally generated by the metabolism of normal cells and plays a crucial role in cell signaling, in liver diseases, an excessive generation of free radicals occurs, which is not scavenged by the antioxidant defense mechanism, causing hepatic tissue damage (Chen et al., 2020). Oxidative stress also plays an important role in the CuO NPs-induced liver toxicity (Siddiqui et al., 2013). It was reported that PCA utilizes its antioxidant activity and scavenges the excessive ROS (Kakkar and Bais, 2014). This study also demonstrated that the CuO NPs-induced pro-oxidant generation (ROS and H_2O_2) in liver cells were effectively abrogated by the PCA pre-treatment, which can be associated with the antioxidant activity of PCA. MDA is a major product of membrane lipid peroxidation, and the increased generation of intracellular free radicals can result in overproduction of MDA (Chung et al, 2019). This study showed that the CuO NPs triggered the MDA level in HepG2 and primary rat hepatocytes. Additionally, the pre-treatment of PCA significantly decreased the CuO NPs-induced MDA level, suggesting the anti-lipid peroxidative potential of PCA.

The protective mechanism of PCA against the effects of CuO NPs on the antioxidant defense ability of liver cells was further investigated. GSH is a well-known antioxidant molecule that protects the by the ROS scavenging activity, reduction of peroxides, and restoration of protein thiols in a reduced state (Eteshola et al., 2020). GSH depletion is also known for its association with apoptosis (De Nicola and Ghibelli, 2014). GPx enzyme reduces the lipid peroxides and hydrogen peroxides using GSH as a substrate, producing GSSG. SOD enzyme acts as the first line of defense by converting superactive superoxide anion ($O_2^{\bullet -}$) into H_2O_2. CAT enzyme further catalyzes toxic H_2O_2 into water and molecular oxygen (Gaucher et al., 2018). Our data demonstrated that the CuO NPs exposure significantly decreased the GSH level and activity of GPx, SOD, and CAT enzymes in the liver cells. Interestingly, the depletion of antioxidant levels in liver cells following the CuO NPs exposure was significantly restored by the PCA pre-treatment.

ROS also plays an important role in the signaling pathway of apoptosis by inducing the activation of caspases (Yang et al., 2020). Among all the caspases, caspase-3 is the main executioner caspase that results in the cytoskeleton breakdown and nuclear changes involved in apoptosis (Ahamed et al., 2022a). We observed that the up-regulation of the caspase-3 gene (mRNA) following CuO NPs exposure in liver cells was remarkably alleviated by PCA pre-treatment. Similarly, CuO NPs induced caspase-3 enzyme activity was also mitigated by PCA in HepG2 cells and primary rat hepatocytes. MMP is another reliable marker of stress and

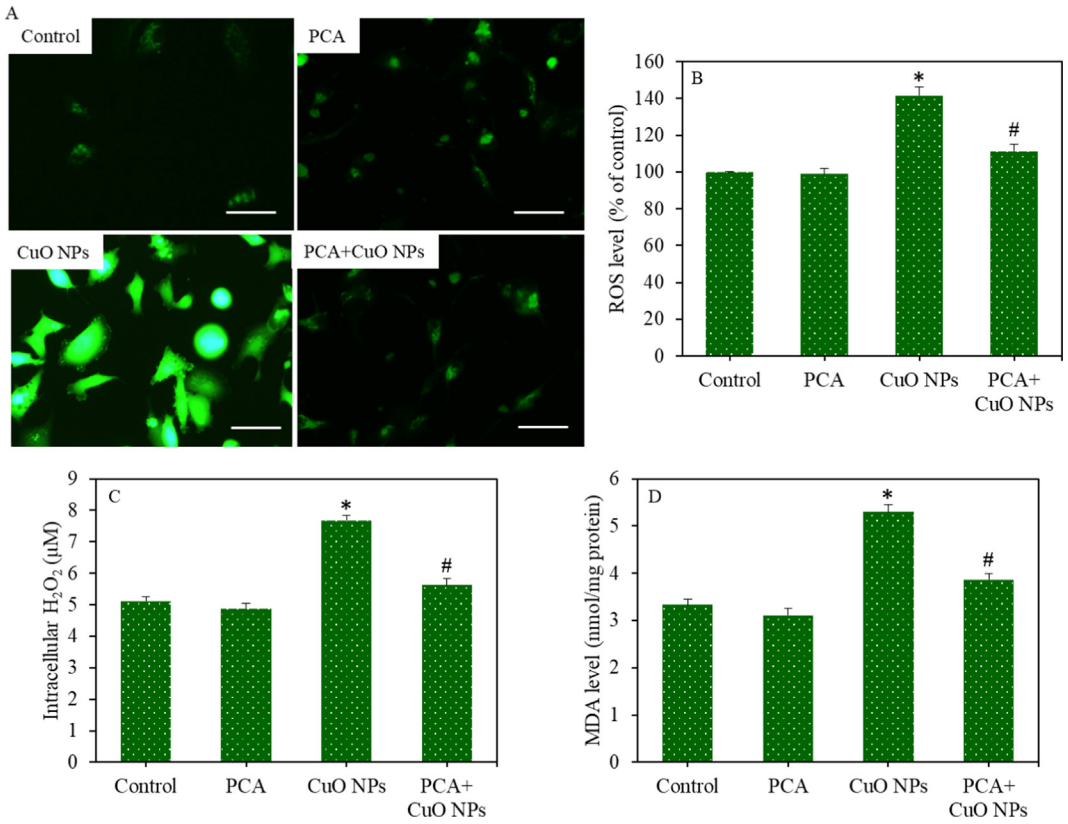

Fig. 3. Pro-oxidants generation in HepG2 cells following exposure to the CuO NPs (IC_{50}) and/or PCA (10 μg/mL) for 24 h. (A) Fluorescent microscope images of intracellular ROS generation (scale bar represents 50 μm). (B) Quantitative analysis of intracellular ROS level. (C) Intracellular H_2O_2 level. (D) MDA level. *statistically significant difference from the control group ($p < 0.05$). #statistically significant difference from the CuO NPs group ($p < 0.05$).

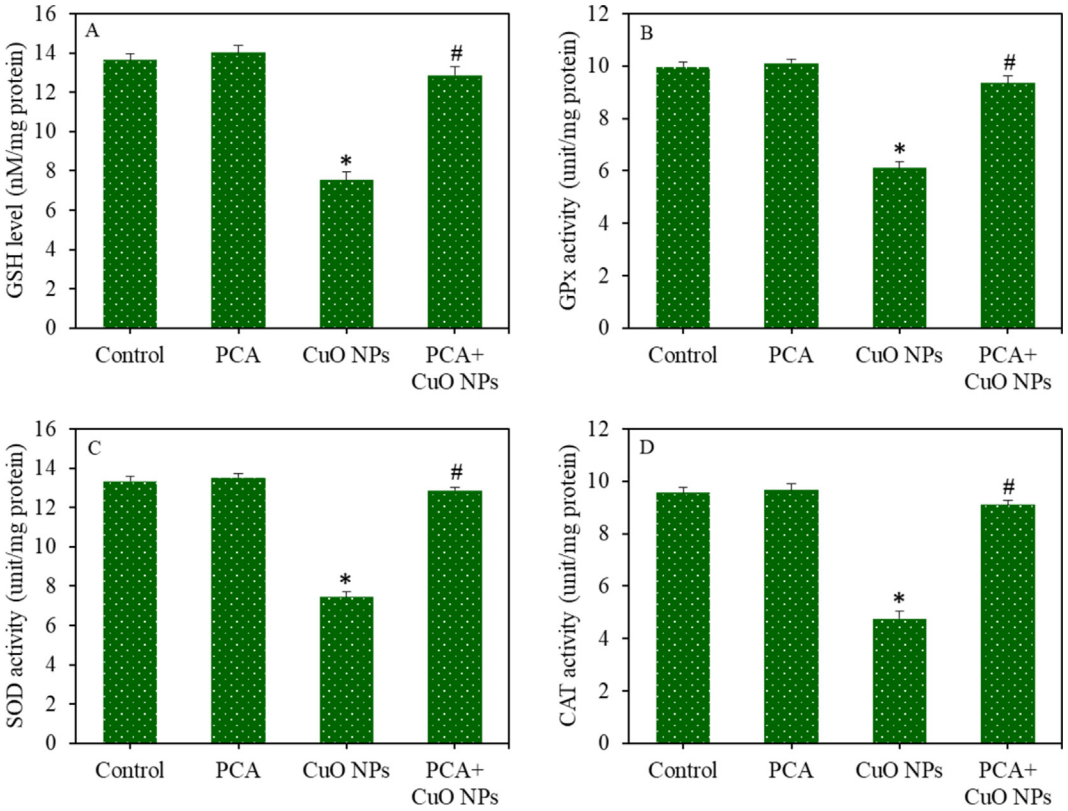

Fig. 4. Antioxidants depletion in HepG2 cells following exposure to the CuO NPs (IC_{50}) and/or PCA (10 μg/mL) for 24 h. (A) GSH level. (B) GPx enzyme activity. (C) SOD enzyme activity. (D) CAT enzyme activity. *statistically significant difference from the control group ($p < 0.05$). #statistically significant difference from the CuO NPs group ($p < 0.05$).

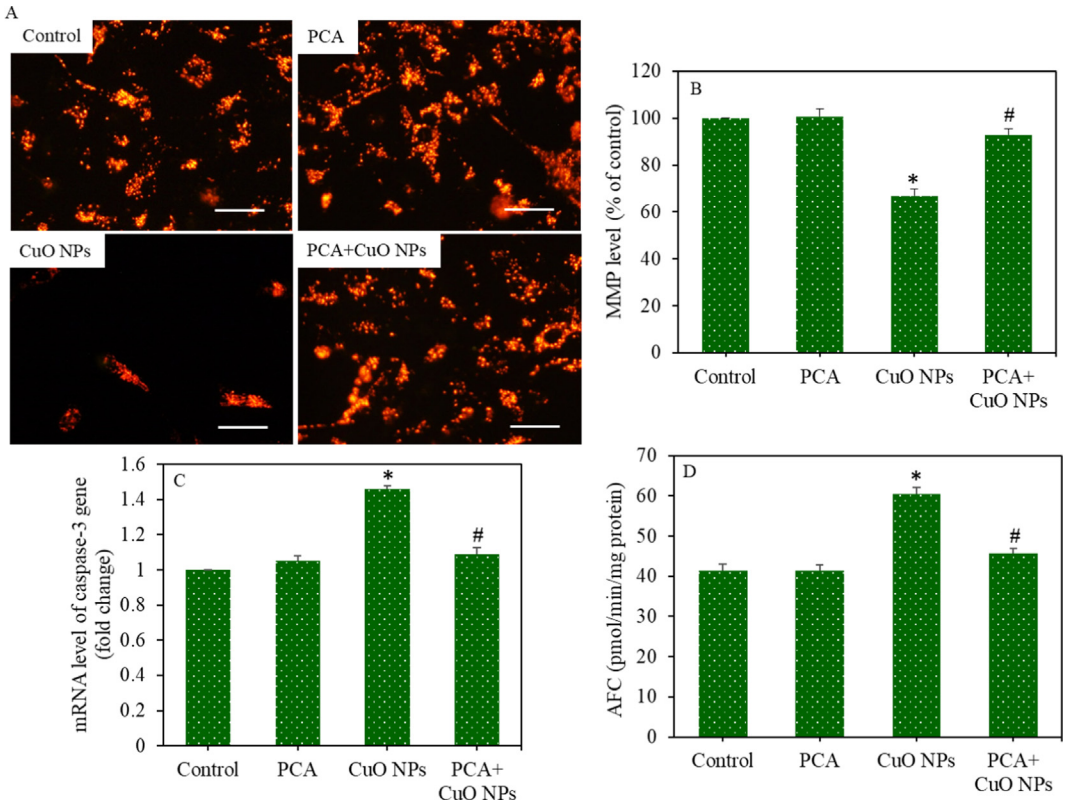

Fig. 5. Apoptotic response of HepG2 cells following exposure to CuO NPs (IC_{50}) and/or PCA (10 µg/mL) for 24 h. (A) Fluorescent microscope images of TMRM (indicator of MMP) (scale bar represents 50 µm). (B) Quantitative analysis of MMP. (C) The mRNA level of caspase-3 gene. (D) Caspase-3 enzyme activity. *statistically significant difference from the control group ($p < 0.05$). #statistically significant difference from the CuO NPs group ($p < 0.05$).

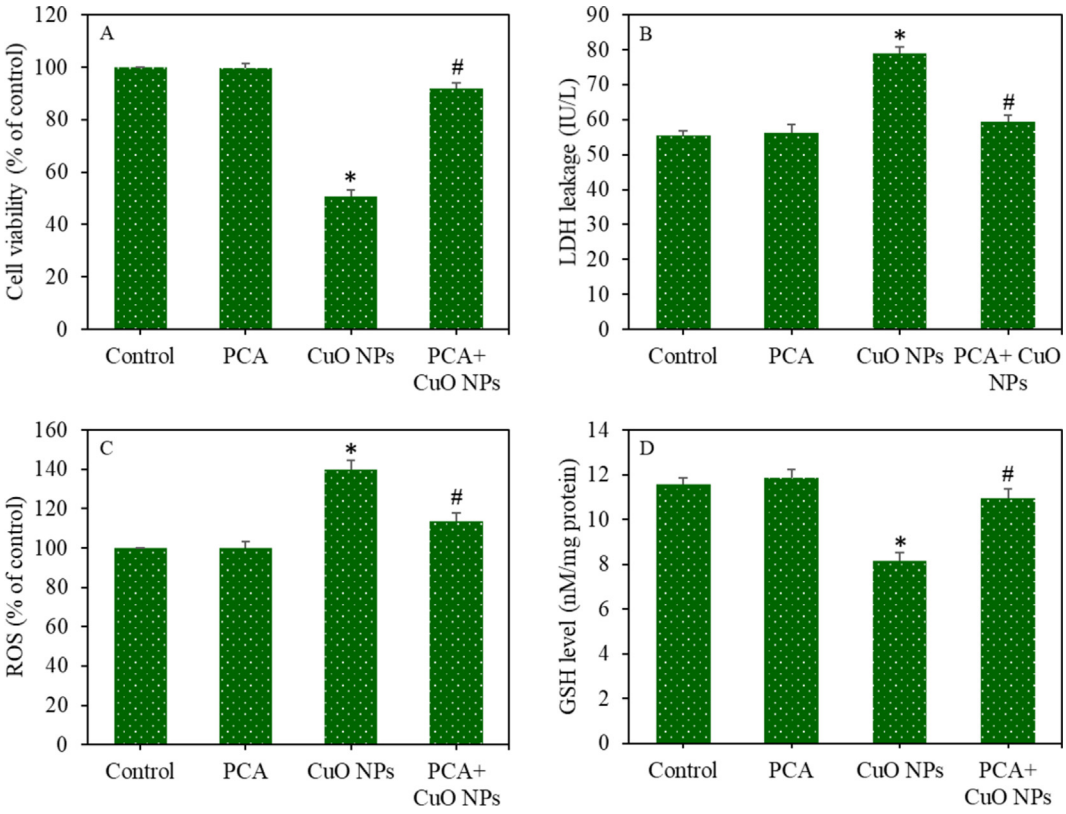

Fig. 6. Cytotoxicity and oxidative stress response of primary rat hepatocytes following exposure to the CuO NPs (IC_{50}) and/or PCA (10 µg/mL for 24 h. (A) MTT cell viability. (B) LDH enzyme leakage. (C) ROS level. (D) GSH level. *statistically significant difference from the control group ($p < 0.05$). #statistically significant difference from the CuO NPs group ($p < 0.05$).

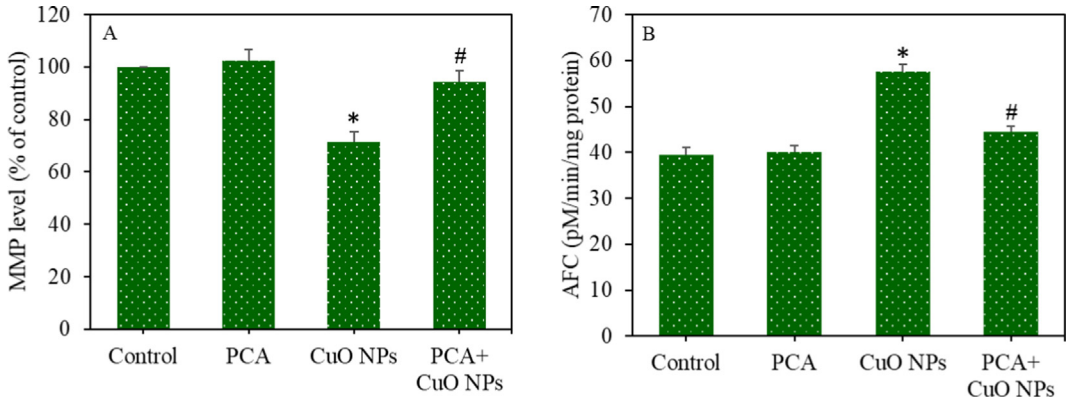

Fig. 7. Apoptotic response of primary rat hepatocytes following exposure to the CuO NPs (IC_{50}) and/or PCA (10 μg/mL) for 24 h. (A) MMP level. (B) Caspase-3 enzyme activity. *statistically significant difference from the control group ($p < 0.05$). #statistically significant difference from the CuO NPs group ($p < 0.05$).

apoptosis. MMP level is depleted during the apoptosis process (Seo et al., 2020). This study showed that CuO NPs induced MMP depletion in HepG2 cells and primary rat hepatocytes was reverted by PCA, suggesting the anti-apoptotic effects of PCA against the CuO NPs-induced apoptosis.

5. Conclusion

In summary, the cytoprotective effect of PCA from CuO NPs toxicity in liver cells was examined. In HepG2 cells and primary rat hepatocytes *in vitro* models, CuO NPs-induced cell viability reduction, LDH leakage, free oxygen radical generation, and antioxidants depletion was remarkably mitigated by PCA. MMP depletion and caspase-3 gene activation by CuO NPs exposure were also successfully reverted by PCA. Conclusively, the present work provides evidence that PCA protects liver cells from CuO NPs toxicity by restoring antioxidants and reducing apoptotic response. This study warrants future research on the mitigating potential of PCA against CuO NPs-induced hepatotoxicity in animal models.

Declaration of Competing Interest

The authors declare that they have no known competing financial interests or personal relationships that could have appeared to influence the work reported in this paper.

Acknowledgment

The authors extend their appreciation to the Deputyship for Research & Innovation, Ministry of Education in Saudi Arabia for funding this research work through the project no. (IFKSURG-2-713).

Appendix A. Supplementary data

Supplementary data to this article can be found online at https://doi.org/10.1016/j.jksus.2023.102585.

References

Abdelazeim, S.A., Shehata, N.I., Aly, H.F., Shams, S.G.E., 2020. Amelioration of oxidative stress-mediated apoptosis in copper oxide nanoparticles-induced liver injury in rats by potent antioxidants. Sci. Rep. 10 (1), 1–14. https://doi.org/10.1038/s41598-020-67784-y.

Abudayyak, M., Guzel, E., Özhan, G., 2020. Cupric oxide nanoparticles induce cellular toxicity in liver and intestine cell lines. Adv. Pharm. Bull. 10 (2), 213–220. https://doi.org/10.34172/apb.2020.025.

Ahamed, M., Akhtar, M.J., Siddiqui, M.A., Ahmad, J., Musarrat, J., Al-Khedhairy, A.A., Alrokayan, S.A., 2011. Oxidative stress mediated apoptosis induced by nickel ferrite nanoparticles in cultured A549 cells. Toxicology 283 (2–3), 101–108. https://doi.org/10.1016/j.tox.2011.02.010.

Ahamed, M., Akhtar, M.J., Alhadlaq, H.A., Alrokayan, S.A., 2015. Assessment of the lung toxicity of copper oxide nanoparticles: current status. Nanomedicine 10 (15). https://doi.org/10.2217/nnm.15.72.

Ahamed, M., Lateef, R., Akhtar, M.J., Rajanahalli, P., 2022a. Dietary antioxidant curcumin mitigates CuO nanoparticle-induced cytotoxicity through the oxidative stress pathway in human placental cells. Molecules 27, 7378. https://doi.org/10.3390/molecules27217378.

Ahamed, M., Akhtar, M.J., Alhadlaq, H.A., 2022b. Combined effect of single-walled carbon nanotubes and cadmium on human lung cancer cells. Environ. Sci. Pollut. Res. 29, 87844–87857. https://doi.org/10.1007/s11356-022-21933-0.

Akhtar, M.J., Ahamed, M., Alhadlaq, H., 2020. Gadolinium oxide nanoparticles induce toxicity in human endothelial huvecs via lipid peroxidation, mitochondrial dysfunction and autophagy modulation. Nanomaterials 10 (9), 1–18. https://doi.org/10.3390/nano10091675.

AlOlayan, E.M., Aloufi, A.S., AlAmri, O.D., El-Habit, O.H., Abdel Moneim, A.E., 2020. Protocatechuic acid mitigates cadmium-induced neurotoxicity in rats: Role of oxidative stress, inflammation and apoptosis. Sci. Total Environ. 723,. https://doi.org/10.1016/j.scitotenv.2020.137969 137969.

Anreddy, R.N.R., 2018. Copper oxide nanoparticles induces oxidative stress and liver toxicity in rats following oral exposure. Toxicol. Rep. 5, 903–904. https://doi.org/10.1016/j.toxrep.2018.08.022.

Antony, F.M., Wasewar, K., 2020. Reactive extraction: a promising approach to separate protocatechuic acid. Environ. Sci. Pollut. Res. 27 (22), 27345–27357. https://doi.org/10.1007/s11356-019-06094-x.

Arun, L., Karthikeyan, C., Philip, D., Unni, C., 2020. Optical, magnetic, electrical, and chemo-catalytic properties of bio-synthesized CuO/NiO nanocomposites. J. Phys. Chem. Solid 136,. https://doi.org/10.1016/j.jpcs.2019.109155 109155.

Baeg, E., Sooklert, K., Sereemaspun, A., 2018. Copper oxide nanoparticles cause a dose-dependent toxicity via inducing reactive oxygen species in drosophila. Nanomaterials 8 (10). https://doi.org/10.3390/nano8100824.

Bialy, B.E., Hamouda, R.A., Eldaim, M.A.A., El Ballal, S.S., Heikal, H.S., Khalifa, H.K., Hozzein, W.N., 2020. Comparative toxicological effects of biologically and chemically synthesized copper oxide nanoparticles on mice. Int. J. Nanomed. 15, 3827–3842. https://doi.org/10.2147/IJN.S241922.

Bradford, M.M., 1976. A rapid and sensitive method for the quantitation of microgram quantities of protein utilizing the principle of protein-dye binding. Anal. Biochem. 72 (1–2), 248–254. https://doi.org/10.1016/0003-2697(76)90527-3.

Chen, Z., Tian, R., She, Z., Cai, J., Li, H., 2020. Role of oxidative stress in the pathogenesis of nonalcoholic fatty liver disease. Free Radic. Biol. Med. 152, 116–141. https://doi.org/10.1016/j.freeradbiomed.2020.02.025.

Chung, I.M., Rekha, K., Venkidasamy, B., Thiruvengadam, M., 2019. Effect of Copper Oxide Nanoparticles on the Physiology, Bioactive Molecules, and Transcriptional Changes in Brassica rapa ssp. rapa Seedlings. Water Air Soil Pollut. 230 (2), 1–14. https://doi.org/10.1007/s11270-019-4084-2.

De Nicola, M., Ghibelli, L., 2014. Glutathione depletion in survival and apoptotic pathways. Front. Pharmacol. 5, 267. https://doi.org/10.3389/fphar.2014.00267.

Ellman, G.L., 1959. Tissue sulfhydryl groups. Arch. Biochem. Biophys. 82 (1), 70–77. https://doi.org/10.1016/0003-9861(59)90090-6.

Eteshola, E.O.U., Haupt, D.A., Koos, S.I., Siemer, L.A., Morris, D.L., 2020. The role of metal ion binding in the antioxidant mechanisms of reduced and oxidized glutathione in metal-mediated oxidative DNA damage. Metallomics 12 (1), 79–91. https://doi.org/10.1039/c9mt00231f.

Fahmy, H.M., Ebrahim, N.M., Gaber, M.H., 2020. In-vitro evaluation of copper/copper oxide nanoparticles cytotoxicity and genotoxicity in normal and cancer lung cell lines. J. Trace Elem. Med Biol. 60,. https://doi.org/10.1016/j.jtemb.2020.126481 126481.

Gaucher, C., Boudier, A., Bonetti, J., Clarot, I., Leroy, P., Parent, M., 2018. Glutathione: Antioxidant properties dedicated to nanotechnologies. Antioxidants 7, 62. https://doi.org/10.3390/antiox7050062. MDPI AG.

Islam, M.R., Obaid, J.E., Saiduzzaman, M., Nishat, S.S., Debnath, T., Kabir, A., 2020. Effect of Al doping on the structural and optical properties of CuO nanoparticles prepared by solution combustion method: Experiment and DFT investigation. J. Phys. Chem. Solid 147,. https://doi.org/10.1016/j.jpcs.2020.109646 109646.

Kakkar, S., Bais, S., 2014. A review on protocatechuic acid and its pharmacological potential. ISRN Pharmacology 2014, 1–9. https://doi.org/10.1155/2014/952943.

Khalaj, M., Kamali, M., Khodaparast, Z., Jahanshahi, A., 2018. Copper-based nanomaterials for environmental decontamination – An overview on technical and toxicological aspects. Ecotoxicol. Environ. Saf. 148, 813–824. https://doi.org/10.1016/j.ecoenv.2017.11.060. Academic Press.

Lee, I.-C., Ko, J.-W., Park, S.-H., Shin, N.-R., Shin, I.-S., Moon, C., Kim, J.-C., 2016. Comparative toxicity and biodistribution assessments in rats following subchronic oral exposure to copper nanoparticles and microparticles. Part. Fibre Toxicol. 13 (1), 56. https://doi.org/10.1186/s12989-016-0169-x.

Moldéus, P., Högberg, J., Orrenius, S., 1978. Isolation and use of liver cells. Methods Enzymol. 52 (C), 60–71. https://doi.org/10.1016/S0076-6879(78)52006-5.

Moschini, E., Gualtieri, M., Colombo, M., Fascio, U., Camatini, M., Mantecca, P., 2013. The modality of cell-particle interactions drives the toxicity of nanosized CuO and TiO_2 in human alveolar epithelial cells. Toxicol. Lett. 222 (2), 102–116. https://doi.org/10.1016/j.toxlet.2013.07.019.

Mosmann, T., 1983. Rapid colorimetric assay for cellular growth and survival: application to proliferation and cytotoxicity assays. J. Immunol. Methods 65 (1–2), 55–63. https://doi.org/10.1016/0022-1759(83)90303-4.

Ohkawa, H., Ohishi, N., Yagi, K., 1979. Assay for lipid peroxides in animal tissues by thiobarbituric acid reaction. Anal. Biochem. 95 (2), 351–358. https://doi.org/10.1016/0003-2697(79)90738-3.

Owumi, S.E., Ochaoga, S.E., Odunola, O.A., Farombi, E.O., 2019. Protocatechuic acid inhibits testicular and epididymal toxicity associated with methotrexate in rats. Andrologia 51 (9). https://doi.org/10.1111/and.13350.

Rotruck, J.T., Pope, A.L., Ganther, H.E., Swanson, A.B., Hafeman, D.G., Hoekstra, W.G., 1973. Selenium: Biochemical role as a component of glatathione peroxidase. Science 179 (4073), 588–590. https://doi.org/10.1126/science.179.4073.588.

Semaming, Y., Pannengpetch, P., Chattipakorn, S.C., Chattipakorn, N., 2015. Pharmacological properties of protocatechuic acid and its potential roles as complementary medicine. Evid. Based Complement. Alternat. Med. 2015,. https://doi.org/10.1155/2015/593902 593902.

Seo, S.U., Woo, S.M., Kim, M.W., Lee, H.-S., Kim, S.H., Kang, S.C., Kwon, T.K., 2020. Cathepsin K inhibition-induced mitochondrial ROS enhances sensitivity of cancer cells to anti-cancer drugs through USP27x-mediated Bim protein stabilization. Redox Biol. 30,. https://doi.org/10.1016/j.redox.2019.101422 101422.

Siddiqui, M.A., Alhadlaq, H.A., Ahmad, J., Al-Khedhairy, A.A., Musarrat, J., Ahamed, M., 2013. Copper oxide nanoparticles induced mitochondria mediated apoptosis in human hepatocarcinoma cells. PLoS One 8 (8). https://doi.org/10.1371/journal.pone.0069534.

Sinha, A.K., 1972. Colorimetric assay of catalase. Anal. Biochem. 47 (2), 389–394. https://doi.org/10.1016/0003-2697(72)90132-7.

Welder, A.A., 1992. A primary culture system of adult rat heart cells for the evaluation of cocaine toxicity. Toxicology 72 (2), 175–187. https://doi.org/10.1016/0300-483X(92)90111-Q.

Yang, Y., Song, Z., Wu, W., Xu, A., Lv, S., Ji, S., 2020. ZnO quantum dots induced oxidative stress and apoptosis in HeLa and HEK-293T cell lines. Front. Pharmacol. 11, 131. https://doi.org/10.3389/fphar.2020.00131.